Electrochimica Acta 427 (2022) 140841

Contents lists available at ScienceDirect

Electrochimica Acta

journal homepage: www.journals.elsevier.com/electrochimica-acta

A roadmap for hydrogel-based quasi-solid electrolyte preparation for use in dye-sensitized solar cell

Mücella Özbay Karakuş [a], Merve Eren Yakışıklıer [b], Ali Delibaş [c], Hidayet Çetin [d,*]

[a] Department of Computer Engineering, Engineering and Architecture Faculty, Yozgat Bozok University, Yozgat 66100, Turkey
[b] Sorgun Vocational School, Yozgat Bozok University, Yozgat 66700, Turkey
[c] Department of Chemistry, Art & Science Faculty, Yozgat Bozok University, Yozgat 66100, Turkey
[d] Department of Physics, Art & Science Faculty, Yozgat Bozok University, Yozgat 66100, Turkey

ARTICLE INFO

Keywords:
Dye-sensitized solar cell
Quasi-solid electrolyte
Hydrogel electrolyte

ABSTRACT

Although the use of quasi-solid electrolytes in dye-sensitized solar cells (DSSCs) is viewed as a solution to the stability problem of DSSCs, the network structure effect on the DSSCs' performance has not been studied in detail. Structurally different hydrogels poly (2-methacryloyloxyethyl trimethylammonium chloride-co-acrylic acid) were prepared and used as quasi-solid gel electrolytes in DSSCs to investigate the network structure effect of hydrogels on DSSC performance. The hydrogel's network structure was changed using different amounts of cross-linkers during synthesis. Five quasi-solid electrolytes were prepared from the hydrogels. The increased cross-linking of quasi-solid electrolytes during synthesis raised conductivity from 0.102 to 0.144 S m^{-1}. Despite expectations, it was observed that the energy conversion efficiency of DSSCs does not follow the rising trend in conductivity, as it rises from 6.57% to 6.62% and then decreases to 5.17%, with increased cross-linking. Moreover, cross-linking during hydrogel synthesis defines not only the electrical properties of quasi-solid electrolytes but also the swelling, wetting, and morphological properties of the structure. Therefore, this study aimed to investigate how and which parameters affect the energy conversion efficiency of DSSCs that are prepared with quasi-solid electrolytes.

1. Introduction

When global warming started to threaten living life, environmentalist approaches came to the forefront in all production areas. Countries planned to replace traditional energy generation strategies with green energy ones [1], and plans were made to evolve fossil-fuel-consuming vehicles into electric ones [2]. In addition to the increased need for electricity, depending on the developing industry, electric cars will require more energy. Solar cells have gained a commercial place in electric energy production due to their environmental characteristics. Although solar cells have proved themselves with their electricity generation, research on solar cells is ongoing. The researchers' goal is to produce solar cells with superior features and cheaper and easier production steps. In addition to the widespread use of silicon-based solar cells, research on perovskite [3,4] and dye-sensitized solar cells (DSSCs) continues intensively [5,6]. While perovskite solar cells stand out with their relatively higher energy conversion efficiency, DSSCs draw attention with their power generation in low-light conditions and indoor usage [7]. Therefore, the broader use of the different types of solar cells according to the needs in low-light conditions or outdoor lighting will reduce the likelihood of environmental disasters due to global warming. DSSCs come to the forefront due to their ability to generate electricity at low light intensities and their easy and relatively cheap fabrication [8,9]. However, widespread commercial demands on DSSCs depend on the stability and lifetime of DSSCs [10,11]. The use of liquid electrolytes in DSSCs brings the possibility of leakage or volatilization problems [12–15]. These problems reduce the reliability of DSSCs and quasi-solid electrolytes could be a solution for the stability problem [16–18].

When the liquid electrolyte trapped gel polymer matrix is used in DSSCs, electrolyte leakage will be prevented, even if the cell receives an impact. According to the literature, many studies use quasi-solid-gel electrolytes in DSSCs [19–24]. Moreover, quasi-solid gel electrolytes are formed with a wide variety of polymers and successfully applied in DSSCs [25,26]. However, studies using hydrogels are quite limited. Hydrogels are defined as a kind of polymeric material that can swell in liquid without dissolving. Unlike other polymers, hydrogels with 3D

* Corresponding author.
E-mail address: hidayet.cetin@bozok.edu.tr (H. Çetin).

https://doi.org/10.1016/j.electacta.2022.140841
Received 4 April 2022; Received in revised form 7 July 2022; Accepted 10 July 2022
Available online 11 July 2022
0013-4686/© 2022 Elsevier Ltd. All rights reserved.

network structures have a much higher liquid-holding capacity. They can uptake liquid as high as 100,000%. Additionally, they are flexible and have natural, tissue-like properties [27–29]. In the liquid electrolyte environment in a 3D network structure in a hydrogel, ions can move more easily, and the relatively high ion mobility can provide both high energy conversion efficiency and a more effective quasi-solid gel medium. As hydrogels are promising materials for flexible electronics and supercapacitors [30], it is necessary to use them to produce quasi-solid gel electrolytes and investigate the subject in more detail. The common point during the synthesis of hydrogels is the use of cross-linkers. The mechanical properties of hydrogels could depend on the cross-linking structure that determines the hydrogels' properties [31]. In addition to the change of mechanical properties with cross-linking, changes to the electrical properties of the hydrogels could be expected. The use of hydrogels in DSSC that were prepared using different amounts of cross-linkers should be analyzed in detail. To this end, the work was processed using five cross-linking ratio-modulated cationic poly (2-methacryloyloxyethyl trimethylammonium chloride-co-acrylic acid) hydrogels (KJ04, KJ06, KJ08, KJ10, and KJ12).

2. Materials and methods

2.1. Preparation of the hydrogels

Several hydrogels were prepared using free-radical polymerization in an aqueous medium. During the synthesis of the hydrogels, the monomer ratios of the *2-methacryloyloxyethyl trimethylammonium chloride* (Q-DMC) and *acrylic acid* (AA) were kept constant as 0.5, and the *N, N methylene bisacrylamide* cross-linker ratios were changed to 0.4, 0.6, 0.8, 1.0, and 1.2. The hydrogels that were produced were labeled as KJ04, KJ06, KJ08, KJ10, and KJ12 in reference to the number of cross-links that were reacted during the synthesis. AA was used without neutralization throughout all the studies. Pre-determined amounts of the monomers and cross-linkers were weighted and solved in deionized water and placed into the falcon tubes. Polymerization was achieved at 55°C for 16 hrs. The hydrogels were cut into small pieces after polymerization and washed with water to remove unreacted monomers. After drying in an oven at 55 °C until they attained a consistent weight, the synthesized hydrogels were stored in covered containers after being ground with a ceramic-head grinder.

2.2. Preparation of the quasi-solid gel electrolytes for the electrical measurements and their use in DSSCs

The quasi-solid gels were formed by impregnating the liquid electrolytes into the hydrogels. HI30 purchased from Solaronix was used as a liquid electrolyte. The hydrogels that were produced were kept in the liquid electrolyte for five days to ensure sufficient liquid absorption. After this time, the unabsorbed liquid electrolytes were filtered to obtain a quasi-solid electrolyte.

For dielectric measurements, quasi-solid electrolyte pellets were used. For this purpose, 300 mg for each KJ04, KJ06, KJ08, KJ10, and KJ12 hydrogel powder were pelleted under 6 tons of pressure. Pellets with a diameter of 12.8 mm and a thickness of approximately 1.9 mm were obtained, and 10 mL of liquid electrolytes were added to each pellet. After they were kept in the liquid electrolytes, unabsorbed part of the liquid electrolyte filtered and the weights of the pellets were measured. Additionally, the liquid electrolytes' holding capacities and the wetting characteristics of the hydrogels were tested by standing them on paper sheets in the atmospheric environment at room temperature.

The electrochemical impedance spectroscopy (EIS) measurements of the dry hydrogel pellets and quasi-solid gel electrolytes were obtained using an Agilent 4284A LCR meter and 16451-B text fixture using the parallel plate capacitor technique to characterize the conductivities and dielectric properties of the samples. The frequency scan was set from 20 Hz to 1 MHz by applying a 10 mV AC oscillator signal throughout the experiments for each polymer pellet and quasi-solid gel electrolyte.

2.3. Preparation of the DSSCs

TiO_2 photo electrodes were prepared as mentioned in [32] on an active square area of 0.25 cm^2 (5 × 5 mm^2) and sintered at 450°C. Then, the TiO_2 film thickness of ~11 μm was measured using a profilometer. When the electrodes were cooled in approximately 50-60°C after the sintering procedure, they were immersed in the 0.5 mM ethanolic dye solution for 18 h at room temperature in dark conditions, which was prepared with Ruthenizer 535-bisTBA (N719). Predrilled platinum electrodes were sintered at 420°C for 15 min and sandwiched with photo electrodes using a double layer of Meltonix 1170-60 coded 60 μm thick hot-melt sealing film after adding the polymer gels, which were swelled using Iodolyte HI-30 liquid electrolytes. Platinum electrodes and Meltonix 1170-60 were obtained from Solaronix, and the other chemicals were obtained from Merck. Six DSSCs were prepared, one of which was with the standard liquid electrolyte, and the others were with quasi-solid gels that were prepared using different amounts of cross-linkers. Three samples were fabricated for each DSSC type to question the experiment's reproducibility and minimize experimental errors.

2.4. Electrical characterization of DSSCs

The current-applied potential (I-V) measurements of the DSSCs were performed under 1,000 W m^{-2} AM1.5 illumination intensity using Science Tech SLB-300A.

The Nyquist plots of the DSSCs were performed using VersaSTAT 3 Potentiostat Galvanostat in dark conditions at room temperature in a Faraday cage. An AC oscillator signal was applied at the amplitude of 10 mV. The frequency range was applied from 10 mHz to 1 MHz for all samples. The Nyquist plots of the DSSCs were fitted using the equivalent circuit, which is provided in the inset of Fig. 6 using the ZView program.

3. Results

3.1. Morphological properties of hydrogels

Fig. 1 depicts the effect of cross-linking on the hydrogel structure. The cross-links are shown with red in the network. Adding cross-links changes the network's structure and the electrical properties of the hydrogels due to the connecting chains. Fig. 2 presents the electrolyte-impregnated hydrogels. The first column shows photos of the quasi-solid electrolytes. Before taking photographs of the samples, the same number of hydrogels and liquid electrolytes were mixed. To ensure adequate electrolyte absorption, the pictures were obtained five days later. Hydrogels with low cross-linking showed a relatively flatter surface. Rougher surfaces were encountered as the ratio increased. In particular, the KJ12 hydrogel reveals a much more irregular surface. In the second column, the surface roughness became more noticeable due to the contour plot, which is a kind of photo transformation of the first column. The light reflection scale was shown next to the photos. After the transformation, deep pits appeared for the lower cross-linker used gels. The swells, which were smaller and more frequent, became sparser and more prominent with the increasing number of cross-links. Adding cross-links between polymer chains affects the physical and morphological properties of the polymer with the presence and absence of crystallinity. As the number of cross-links increases, the polymer becomes more rigid and cannot stretch as much; the polymer will become less viscous and elastic and might even become brittle. An apparent correlation can be established between the morphology of hydrogels with the various cross-linking degrees and this transition in the swelling behavior [33,34].

The third column in the photographs was obtained by depositing the electrolyte-impregnated hydrogels onto white paper and then lifting

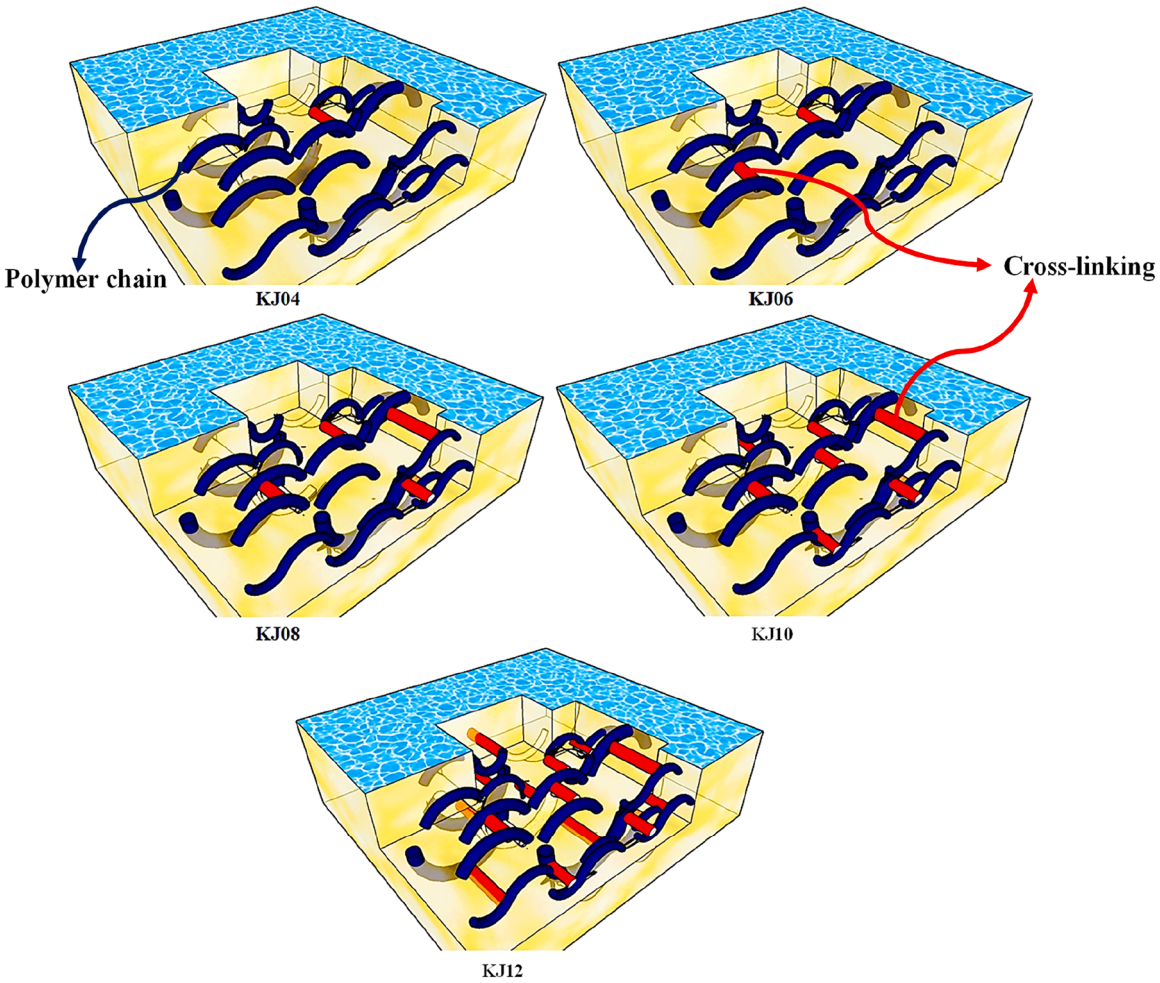


Fig. 1. Schematic diagrams of the hydrogels' cross-linking (For interpretation of the references to color in this figure, the reader is referred to the web version of this article.).

them. The liquid electrolyte stains in the picture provide information about the interaction between the hydrogel and contact surface, the electrolyte-holding capacity of the hydrogels, and releasing the liquid electrolyte. Due to the creamy structure of the hydrogel electrolyte, a perfect contact characteristic could be expected for all the cavities and pits. However, the gel electrolytes that were prepared with KJ04, KJ06, and KJ08 hydrogels left fewer liquid electrolyte traces due to their morphological properties, such as deep pits. Leaving traces on the entire surface is vital because charge carriers will pass through areas that are in contact with DSSC electrodes. The data proves that the necessary properties of the hydrogel for use in DSSCs can be controlled by the usage number of cross-links during synthesis.

Fig. 3's data was obtained after mixing the dry polymers KJ04, KJ06, KJ08, KJ10, and KJ12 with equal amounts of the electrolyte. After resting them in the electrolyte for five days to ensure sufficient electrolyte absorbance, the excess electrolytes that were not absorbed were removed from the medium. The graph shows the effect of the amount of cross-linking on the electrolytes' entrapment ability. The first data in the graph is the hydrogel disc diameter. The hydrogel system expands in diameter as it absorbs the liquid-electrolytes. KJ10 exhibits the largest disk diameter.

Similarly, the disc thickness variations are shown in the graph. The thickest disks are KJ10 and KJ12. The more electrolytes it absorbs, the larger its diameter and the greater its thickness. Moreover, as shown in Fig. 2, cracked and hollow structures may be encountered with excess electrolyte adsorption. In addition, the graph shows the weights of the hydrogels that were impregnated with the liquid electrolyte. When the graphic data was evaluated, it was found that KJ10 and KJ12 were the two structures that absorbed the most liquid electrolyte.

3.2. Electrical properties of the hydrogels

In addition to examining the morphological properties, impedance analyses of all quasi-solid electrolytes were performed. Fig. 4 shows the Nyquist plot of the KJ04 sample. R_b bulk resistances could be determined from the Nyquist plot of samples [35]. The conductivity of the samples was calculated using the area (A) and thickness (t) of the samples from the following equation [36]:

$$\sigma = \frac{t}{AR_b} \tag{1}$$

The calculation results are presented in Fig. 5 for all quasi-solid electrolytes. As shown in Fig. 5, the electrical conductivity increased with the increasing cross-linking of the hydrogels. This may be due to the increased liquid electrolyte absorption and cross-linking. In polymers, the electrical conductivity is mainly realized by the movement of charge carriers along the chains, and the possibility of charge carrier movement between the chains increases electrical conductivity [37]. As shown in Fig. 1, additional cross-links are shown between the chains. The additional cross-links create other pathways for the current transport. Therefore, electrical conductivity increases as cross-links increase.

On the other hand, the idea that higher conductivity quasi-solid electrolyte production can be improved by increasing cross-linking should be questioned for DSSCs. In addition to increased cross-linking

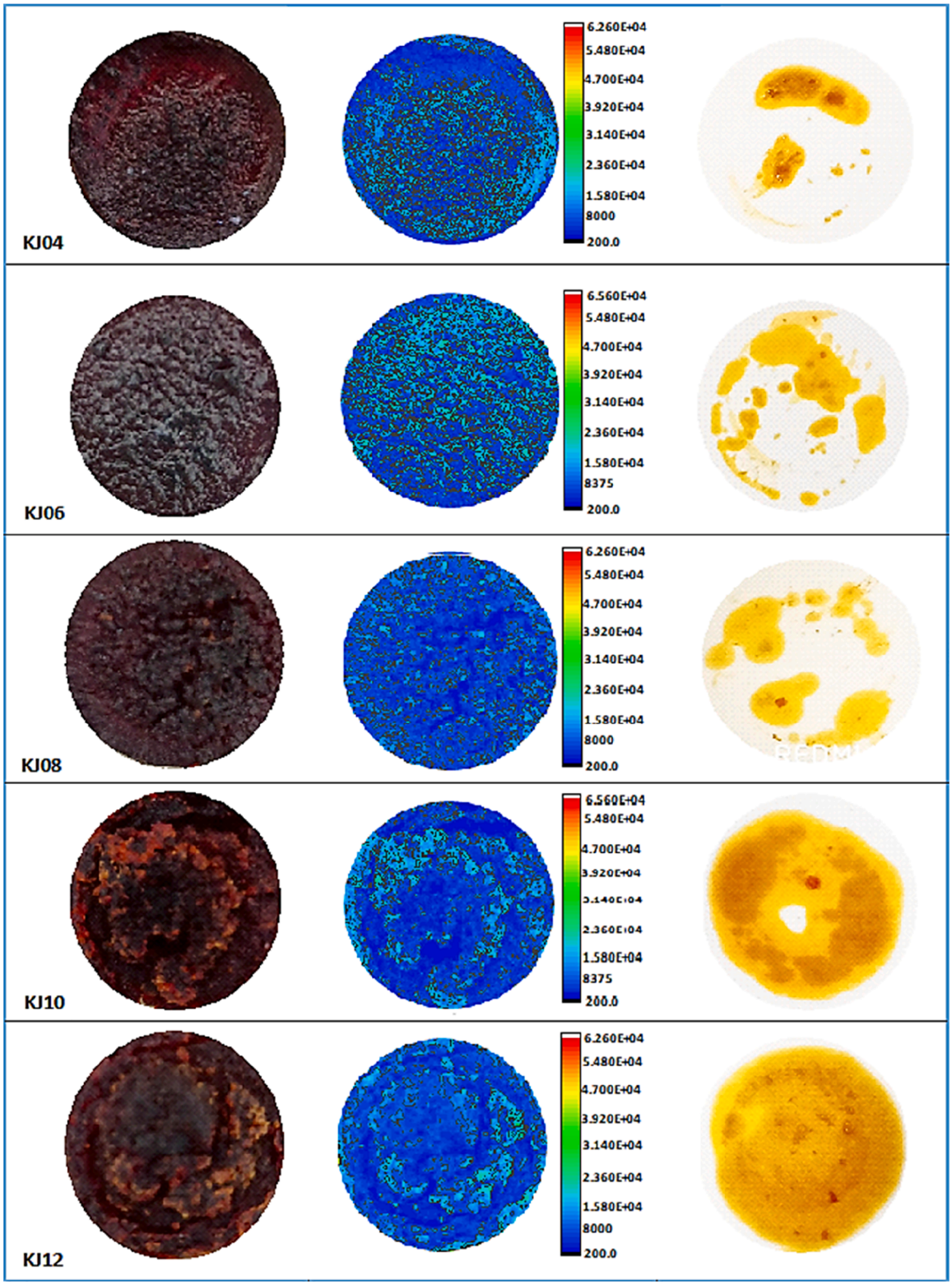


Fig. 2. The first column is the images of the quasi-solid electrolytes, the second column shows the contour plots of the first column and the third is for electrolyte holding capacities of quasi-solid electrolytes.

causing increased conductivity, it could change the properties of hydrogels. Dielectric spectroscopy is a powerful technique to investigate the material properties and charge polarization [38,39]. Table 1 shows the real parts of the dielectric constant of the hydrogels and quasi-solid electrolytes at the 1 kHz frequency. The real parts of the dielectric constant were obtained from non-electrolyte-impregnated hydrogels in the first column, and the data in the second column comes from the quasi-solid electrolyte. The real part of the dielectric constant is defined as a measure of the polar structure in the material [40–42]. As shown in the first column, the polar structure of the hydrogels increased alongside cross-linking. When the data in Fig. 3 is evaluated together with Table 1, increased liquid electrolyte absorption is observed because of the

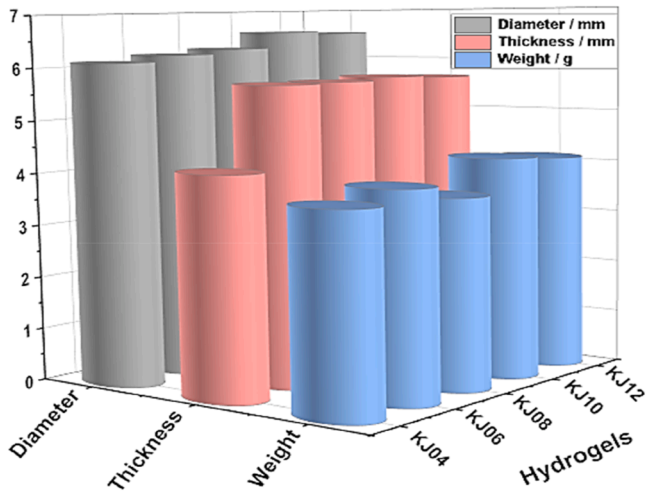


Fig. 3. Graph of the variation in the disc diameter, the disc thickness and the weights of the quasi-solid electrolytes.

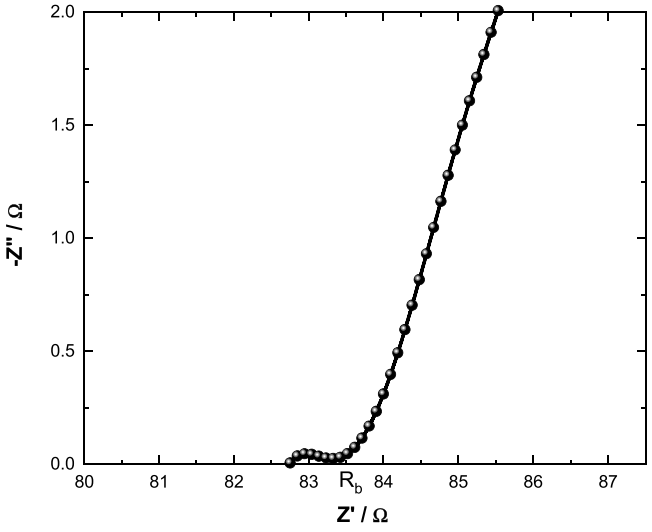


Fig. 4. Real impedance (Z') versus imaginary impedance (Z'') graph of the KJ04 to determine the R_b bulk resistance.

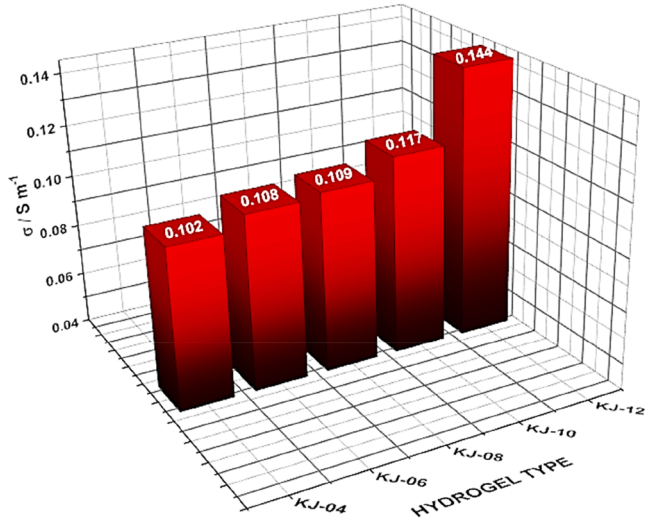


Fig. 5. Conductivities of the quasi-solid electrolytes.

Table 1
The real part of dielectric permittivity of the hydrogels and quasi-solid electrolyte pellets at 1 KHz.

Hydrogel	ε' (Hydrogel pellet)	ε' (Quasi-solid electrolyte)
KJ04	7.88	743.8
KJ06	9.16	692.4
KJ08	10.03	806.3
KJ10	10.05	905.6
KJ125	11.96	1021.2

increased polarity. Moreover, when the KJ10 and KJ12 gels in Fig. 3 were compared in terms of weight, diameter, and thickness, the more polar KJ12 gel absorbed fewer electrolytes. The decreasing elasticity of the hydrogel with increased cross-linking could limit the absorbance of the liquid electrolytes and eliminate the trend between hydrogel polarity and liquid electrolyte absorbance. These results support the idea of a liquid electrolyte absorbance limitation mechanism. Additionally, a more cracked and rougher surface due to the loss of elasticity of the hydrogels with increased cross-linking is shown in Fig. 2. In addition, the swelling properties, which usually use the degree of swelling to define hydrogels, depend on many factors such as network density, solvent nature, polymer-solvent interaction parameter [43]. A cross-linked polymer hydrogels swell but do not dissolve when a solvent enters it. On a molecular level, a polar solvent in a hydrogel either bonds to polar hydrophilic groups or fills the space between the network chains, pores, or voids [44]. The hydrophilic group on the polymer chain holds the polar solvent molecule via Van der Waals attraction and hydrogen bonding [45].

3.3. Photovoltaic performance of hydrogels

To explore the potential of quasi-solid electrolytes for photovoltaic application, DSSCs were measured at AM 1.5. Fig. 6 shows the current-voltage characteristics of the fabricated cells, and the results are summarized in Table 2. The fill factor (FF) and energy conversion efficiency $\eta(\%)$ were calculated using the following equations:

$$FF = \frac{V_{max} x J_{max}}{V_{oc} x J_{sc}} \quad (2)$$

$$\eta(\%) = \frac{V_{oc} x J_{sc} x FF}{P_{in}} \quad (3)$$

where J_{max} and V_{max}, represent the photocurrent density and voltage at the maximal power output point in *J–V* curve, respectively, V_{oc} and J_{sc}

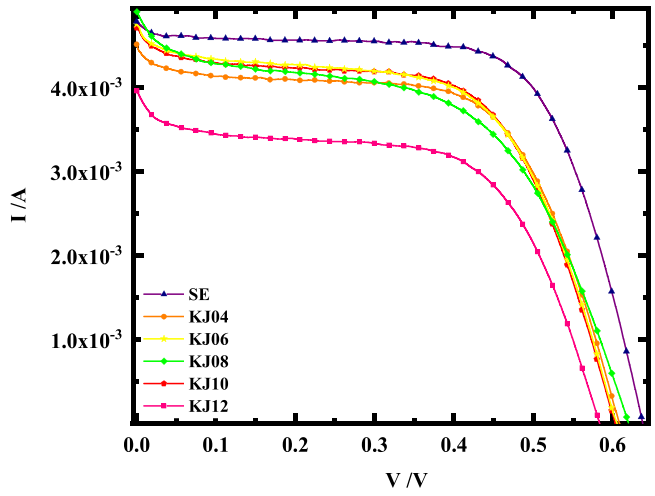


Fig. 6. Applied potential *vs.* current measurements of the DSSCs based on the standard liquid electrolyte (SE) and quasi-solid electrolytes.

Table 2
Performance parameters of the DSSCs.

Used Electrolyte Type	V_{OC} / mV	J_{SC} / mA cm^{-2}	FF	η / %
Liquid Electrolyte (SE)	638 ± 2	18.8 ± 0.3	0.67 ± 0.01	8.05 ± 0.2
KJ04	608 ± 3	17.5 ± 0.1	0.62 ± 0.01	6.57 ± 0.1
KJ06	605 ± 4	18.5 ± 0.3	0.59 ± 0.01	6.59 ± 0.2
KJ08	620 ± 2	19.0 ± 0.1	0.53 ± 0.03	6.21 ± 0.2
KJ10	603 ± 4	18.4 ± 0.2	0.60 ± 0.02	6.62 ± 0.1
KJ12	583 ± 1	15.2 ± 0.4	0.58 ± 0.01	5.17 ± 0.3

are the open-circuit voltage and short-circuit current density, respectively, and P_{in} is the incident light power.

As shown in Table 2, while the cells that used liquid electrolytes exhibited the best performance with 8.05%, the cells that used quasi-solid electrolytes showed values that were relative to the liquid electrolytes that were used. Although it had the highest electrical conductivity, the cell that used KJ12 gel provided the smallest energy conversion efficiency. For a more detailed analysis, the EIS measurements of the produced solar cells were performed. Fig. 7 shows the Nyquist plots of the DSSCs that were measured in dark conditions. The equivalent circuit is presented as an inset. Three semicircles are observed in the graph. The first semicircle region in the high-frequency region is related to the charge-transfer process, which occurred at the Pt counter electrode (R_{pt}). The second semicircle region occurred at the TiO_2/dye/electrolyte interface (R_{ct}), and the third semicircle region corresponds to the diffusion in the gel polymer electrolyte [35,46]. The charge-transfer parameters were obtained from the fitted impedance plots. The results are shown in Table 3. In Table 3, the values of the series resistance R_S of all the samples are very close to each other, as the main contribution to the series resistance comes from the sheet resistance [47]. In addition, the charge recombination resistance R_{pt} increased with the number of cross-links. However, the KJ10 gel disrupts this trend. The increasing electrical conductivity of the gel does not reduce the electrical resistance of the platinum-gel electrolyte interface. The same situation was observed in the R_{ct} resistance, which defines the charge transfer of the TiO_2/gel electrolyte interface. Although the highest R_{ct} value belonged to the DSSC using KJ12 gel, no proportional relationship was observed between the cross-linking or the conductivity of the gel that was used and R_{ct}. This indicates that the mechanism is

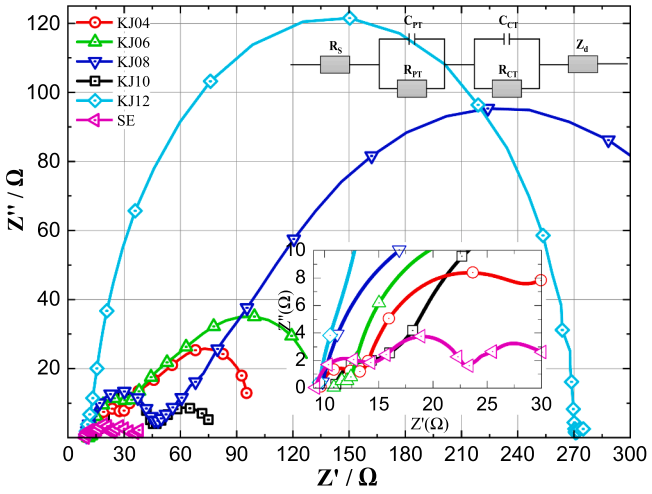


Fig. 7. Nyquist plots of the DSSCs under dark condition. Inset: The equivalent circuit for the DSSCs.

Table 3
The equivalent circuit parameters of the DSSCs based on Nyquist plots.

DSSC (Electrolyte Type)	R_S / Ω	R_{PT} / Ω	C_{PT} / F	R_{CT} / Ω	C_{CT} / F
SE	9.4	8.7	0.3×10^{-3}	4.8	6.9×10^{-6}
KJ04	9.8	14.2	0.4×10^{-3}	3.8	10.3×10^{-6}
KJ06	11.0	17.6	0.8×10^{-3}	3.3	9.1×10^{-6}
KJ08	9.7	79.8	0.9×10^{-3}	34.5	22.8×10^{-6}
KJ10	10.8	27.9	9.7×10^{-3}	7.2	3.7×10^{-6}
KJ12	9.5	125.5	11.4×10^{-6}	116.9	16.0×10^{-6}

more complex in the solar cell using quasi-solid electrolyte. The quasi-solid electrolytes' electrical conductivity and physical contact characteristics also change with the number of cross-links changing. When the quasi-solid electrolytes are sandwiched between the counter electrode and photo anode TiO_2 surface, the morphological structure of the quasi-solid electrolyte and porous structured TiO_2 surface wetting with the liquid electrolyte define the quality of the contact interfaces. Wetting up to a certain layer with the liquid electrolyte is related to quasi-solid electrolyte characteristic and important for effective flow of charge carriers. It is clearly seen from Fig. 2 that the wetting characteristics of quasi-solid electrolytes are not same.

In addition, when the electrical conductors with different work functions are contacted, an energy barrier appears, depending on the conductors' work function [48,49]. The potential energy barrier defines the charge flow across the contact. The change in the polar structure in the polymer material causes a change in the work function [50–52]. The dielectric constant measurements pointed out a change in the polar structure in Table 1. These impacts change the energy barrier height and cause charge accumulation at the interfaces.

Moreover, as can be seen from Fig. 2, the KJ12 quasi-solid electrolyte reveals a much more irregular surface due to the more solid-like structure. R_{ct} is related to the recombination rate at the TiO_2/dye/quasi-solid gel electrolyte interface [53,54]. Interfacial factors viz. dielectric mismatch, interface shape and size, and anisotropy contribute significantly to the interfacial electrostatics [55]. When the more irregular quasi-solid surface are contacted with TiO_2/dye surface, higher recombination rates may be encountered due to the mentioned interfacial factors.

Therefore, seemingly meaningless changes in R_{pt} and R_{ct} are a result of electrical contact characteristics. The energy conversion efficiency of DSSCs will inevitably be affected by these impacts.

4. Conclusion

In this study, poly (2-methacryloyloxyethyl trimethylammonium chloride-co-acrylic acid) hydrogels were prepared using different amounts of cross-linkers, and they were used in DSSC as quasi-solid electrolytes. It is possible to sort the results obtained from the study into the following items:

i This study shows that the amount of cross-linking during hydrogel production significantly affects the quasi-solid electrolyte's morphological and physical characteristics. By changing the amount of cross-linking, the cracked and porous structures on the quasi-solid electrolytes' surface can be controlled.

ii Changing the number of cross-links changes the absorption of the liquid electrolyte of the hydrogel. The dielectric constant measurements show that the polar–polar interaction is the main factor in the absorption of liquid electrolytes. The amount of cross-linking that increases up to a particular turning point increases liquid electrolytes' absorption. After a certain point, the elasticity of the hydrogel may disappear and the amount of absorbed liquid electrolytes

decreases. However, the amount of liquid electrolyte absorption of the hydrogel does not solely determine the efficiency of the solar cell. A higher solar cell energy conversion efficiency may not be achieved when hydrogels that can absorb larger amounts of liquid electrolytes are used.

iii As the amount of cross-linking increases, the electrical conductivity of hydrogels also increases. However, when these hydrogels are used as the quasi-solid electrolyte between the electrodes that comprise the sandwich structure for DSSC, the interfacial contact, morphological and electrical properties of the quasi-solid electrolyte determine the efficiency of the solar cell.

CRediT authorship contribution statement

Mücella Özbay Karakuş: Investigation, Formal analysis. **Merve Eren Yakışıklıer:** Investigation. **Ali Delibaş:** Resources, Investigation. **Hidayet Çetin:** Methodology, Supervision, Writing – review & editing.

Declaration of Competing Interest

The authors declare that they have no known competing financial interests or personal relationships that could have appeared to influence the work reported in this paper.

Data availability

The authors do not have permission to share data.

Acknowledgment

This work was supported by Yozgat Bozok University Scientific Research Projects Unit. We thank to Yozgat Bozok University (Grant No: 6602c-FEN/19-326) for financial support.

References

[1] D. Gielen, F. Boshell, D. Saygin, M.D. Bazilian, N. Wagner, R. Gorini, The role of renewable energy in the global energy transformation, Energy Strategy Rev. 24 (2019) 38–50.
[2] D. Castelvecchi, Electric cars: the battery challenge, Nature 596 (2021) 336–339.
[3] Q. Lou, H. Li, Q. Huang, Z. Shen, F. Li, Q. Du, M. Jin, C. Chen, Multifunctional CNT: TiO_2 additives in spiro-OMeTAD layer for highly efficient and stable perovskite solar cells, EcoMat 3 (3) (2021) 12099.
[4] C.U. Kim, E.D. Jung, Y.W. Noh, S.K. Seo, Y. Choi, H. Park, M.H. Song, K.J. Choi, Strategy for large-scale monolithic perovskite/silicon tandem solar cell: a review of recent progress, EcoMat 3 (2) (2021) 12084.
[5] W. Song, Z. Bie, W. Yan, J. Zhu, W. Ma, Interfacial engineering of nanostructured photoanode in fiber dye-sensitized solar cells for self-charging power systems, EcoMat 4 (3) (2022) 12177.
[6] M. Jin, H. Li, Q. Lou, Q. Du, Q. Huang, Z. Shen, F. Li, C. Chen, Toward high-efficiency stable 2D/3D perovskite solar cells by incorporating multifunctional CNT: TiO_2 additives into 3D perovskite layer, EcoMat 4 (2) (2022) 12166.
[7] K.L. Wang, Y.H. Zhou, Y.H. Lou, Z.K. Wang, Perovskite indoor photovoltaics: opportunity and challenges, Chem. Sci. 12 (36) (2021) 11936–11954.
[8] B. O'Regan, M. Grätzel, A low-cost, high-efficiency solar cell based on dye-sensitized colloidal TiO_2 films, Nature 353 (1991) 737–740.
[9] M. Grätzel, Photoelectrochemical cells, Nature 414 (2001) 338–344.
[10] J.B. Baxter, Commercialization of dye sensitized solar cells: present status and future research needs to improve efficiency, stability, and manufacturing, J. Vac. Sci. Technol. A 30 (2012), 020801.
[11] S. Mozaffari, M.R. Nateghi, M.B. Zarandi, An overview of the Challenges in the commercialization of dye sensitizedsolar cells, Renew. Sustain. Energy Rev. 71 (2017) 675–686.
[12] N. Shahzad, T. Perveen, D. Pugliese, S. Haq, N. Fatima, S.M. Salman, A. Tagliaferro, M.I. Shahzad, Counter electrode materials based on carbon nanotubes for dye-sensitized solar cells, Renew. Sustain. Energy Rev. 159 (2022), 112196.
[13] S. Balamurugan, S. Ganesan, S. Kamaraj, V. Mathew, J. Kim, N. Arumugam, A. I. Almansour, Effect of poly (ethylene glycol) gel polymer electrolyte consist of novel heteroleptic cobalt redox shuttle and pyridine based organic additive on performance of dye sensitized solar cells, Opt. Mater. 125 (2022), 112082.
[14] N.K. Farhana, N.M. Saidi, S. Bashir, S. Ramesh, K. Ramesh, Review on the revolution of polymer electrolytes for dye-sensitized solar cells, Energy Fuels 35 (2021) 19320–19350.
[15] M.H. Jung, Polypyrrole/poly(vinyl alcohol-co-ethylene) quasi-solid gel electrolyte for iodine-free dye-sensitized solar cells, J. Power Sources 268 (2014) 557–564.
[16] P. Wang, S.M. Zakeeruddin, J.E. Moser, M.K. Nazeeruddin, T. Sekiguchi, M. Grätzel, A stable quasi-solid-state dye-sensitized solar cell with an amphiphilic ruthenium sensitizer and polymer gel electrolyte, Nat. Mater. 2 (2003) 402–407.
[17] S. Venkatesan, I.P. Liu, C.W. Li, C. Tseng-Shan, Y.L. Lee, Quasi-solid-state dye-sensitized solar cells for efficient and stable power generation under room light conditions, ACS Sustain. Chem. Eng. 7 (2019) 7403–7411.
[18] T. Önen, M.Ö. Karakuş, R. Coşkun, H. Çetin, Reaching stability at DSSCs with new type gel electrolytes, J. Photochem. Photobiol. A 385 (2019), 112082.
[19] J.K. Lee, M. Yang, Progress in light harvesting and charge injection of dye-sensitized solar cells, Mater. Sci. Eng. B 176 (2011) 1142–1160.
[20] J.N. De Freitas, A.F. Nogueira, M.A. De Paoli, New insights into dye-sensitized solar cells with polymer electrolytes, J. Mater. Chem. 19 (2009) 5279–5294.
[21] F. Bella, R. Bongiovanni, Photoinduced polymerization: an innovative, powerful and environmentally friendly technique for the preparation of polymer electrolytes for dye-sensitized solar cells, J. Photochem. Photobiol. C Photochem. Rev. 16 (2013) 1–21.
[22] R. Khan, M.H. Naveen, J.H. Bang, Similar looks, different photoelectrochemical behavior: unique aspects of metal-nanocluster-sensitized electrodes, ACS Energy Lett. 6 (2021) 2713–2725.
[23] T.M.W.J. Bandara, A.M.J.S. Weerasinghe, M.A.K.L. Dissanayake, G.K.R. Senadeera, M. Furlani, I. Albinsson, B.E. Mellander, Characterization of poly (vinylidene fluoride-co-hexafluoropropylene)(PVdF-HFP) nanofiber membrane based quasi solid electrolytes and their application in a dye sensitized solar cell, Electrochim. Acta 266 (2018) 276–283.
[24] K. Santhosh, S. Ganesan, S. Balamurugan, Novel indole-based photosensitizers coupled with PEG-HEC quasi-solid-state electrolyte to improve energy conversion and stability of organic dyes based-dye sensitized solar cells, Electrochim. Acta 389 (2021), 138771.
[25] U. Mehmood, A. Aslam, M.H. Arshad, A. Ishfaq, J. Zaheer, Mixed cations polymer gel electrolytes for quasi-solid-state dye-sensitized solar cells, IEEE J. Photovolt. 11 (2021) 664–667.
[26] N.M. Saidi, Z.L. Goh, H.M. Arif, N.K. Farhana, S. Ramesh, K. Ramesh, Consolidation of ion promoters into quasi solid-state (QSS) polymer electrolytes for dye-sensitized solar cells (DSSCs), Solid State Ion. 363 (2021), 115592.
[27] F.L. Buchholz, A.T. Graham, Modern Superabsorbent Polymer Technology, John Wiley & Sons Inc., New York, 1998, 605 Third Ave.
[28] L. Brannon-Peppas, R.S. Harland, Absorbent Polymer Technology, Elsevier, Amsterdam, 2012.
[29] M.J.A.D. Zohuriaan-Mehr, K. Kabiri, Superabsorbent polymer materials: a review, Iran. Polym. J. 17 (6) (2008) 451–477.
[30] C.Y. Chan, Z. Wang, H. Jia, P.F. Ng, L. Chow, B. Fei, Recent advances of hydrogel electrolytes in flexible energy storage devices, J. Mater. Chem. A 9 (2021) 2043–2069.
[31] A. Hajikhani, P. Wriggers, M. Marino, Chemo-mechanical modelling of swelling and crosslinking reaction kinetics in alginate hydrogels: a novel theory and its numerical implementation, J. Mech. Phys. Solids 153 (2021), 104476.
[32] M.Ö. Karakuş, M.E. Yakışıklıer, A. Delibaş, E. Ayyıldız, H. Çetin, Anionic and cationic polymer-based quasi-solid-state dye-sensitized solar cell with poly (aniline) counter electrode, Sol. Energy 195 (2020) 565–572.
[33] J. Maitra, V.K. Shukla, Cross-linking in hydrogels-a review, Am. J. Polym. Sci. 4 (2) (2014) 25–31.
[34] R. da Silva, M.G. de Oliveira, Effect of the cross-linking degree on the morphology of poly (NIPAAm-co-AAc) hydrogels, Polymer 48 (14) (2007) 4114–4122.
[35] M.H. Buraidah, S. Shahan, L.P. Teo, F.I. Chowdhury, M.A. Careem, I. Albinsson, B. E. Mellander, A.K. Arof, High efficient dye sensitized solar cells using phthaloylchitosan based gel polymer electrolytes, Electrochim. Acta 245 (2017) 846–853.
[36] A.A. Mohamad, Absorbency and conductivity of quasi-solid-state polymer electrolytes for dye-sensitized solar cells: a characterization review, J. Power Sources 329 (2016) 57–71.
[37] K. Davidson, A.M. Ponsonby, Synthesis of crosslinked electrically conductive polymers, Synth. Met. 102 (1999) 1512–1513.
[38] C. Wu, Y. Gao, X. Liang, S.M. Gubanski, Q. Wang, W. Bao, S. Li, Manifestation of interactions of nano-silica in silicone rubber investigated by low-frequency dielectric spectroscopy and mechanical tests, Polymers 11 (2019) 717.
[39] F. Agrebi, N. Ghorbel, A. Ladhar, S. Bresson, A. Kallel, Enhanced dielectric properties induced by loading cellulosic nanowhiskers in natural rubber: modeling and analysis of electrode polarization, Mater. Chem. Phys. 200 (2017) 155–163.
[40] M. Dascalu, S.J. Dünki, J.E.Q. Quinsaat, Y.S. Ko, D.M. Opris, Synthesis of silicone elastomers containing trifluoropropyl groups and their use in dielectric elastomer transducers, RSC Adv. 5 (2015) 104516–104523.
[41] X. Liu, H. Sun, S. Liu, Y. Jiang, Z. Yin, B. Yu, N. Ning, M. Tian, L. Zhang, Dielectric elastomer sensor with high dielectric constant and capacitive strain sensing properties by designing polar-nonpolar fluorosilicone multiblock copolymers and introducing poly(dopamine) modified C.N.T.s, Compos. B Eng. 223 (2021), 109103.
[42] H. Sun, X. Liu, H. Yan, Z. Feng, B. Yu, N. Ning, M. Tian, L. Zhang, The role of dipole structure and their interaction on the electromechanical and actuation performance of homogeneous silicone dielectric elastomers, Polymer 165 (2019) 1–10.
[43] N.A. Peppas, Biomedical Applications of Hydrogels Handbook, Springer Science & Business Media, 2010.
[44] T. Yang, Mechanical and swelling properties of hydrogels, Doctoral dissertation, KTH Royal Institute of Technology, 2012.

[45] N. Pullanjiot, S. Swaminathan, Enhanced electrochemical properties of metal oxide interspersed polymer gel electrolyte for QSDSSC application, Sol. Energy 186 (2019) 37–45.
[46] L. Han, N. Koide, Y. Chiba, T. Mitate, Modeling of an equivalent circuit for dye-sensitized solar cells, Appl. Phys. Lett. 84 (13) (2004) 2333–2435.
[47] R.S. Moraes, E. Saito, D.M.G. Leite, M. Massi, A.S. da Silva Sobrinho, Optical, electrical and electrochemical evaluation of sputtered platinum counter electrodes for dye sensitized solar cells, Appl. Surf. Sci. 364 (2016) 229–234.
[48] A. Vilan, A. Shanzer, D. Cahen, Molecular control over Au/GaAs diodes, Nature 40 (2000) 166–168.
[49] S. Walia, S. Balendhran, Y. Wang, R. Ab Kadir, A. Sabirin Zoolfakar, P. Atkin, J. Z. Ou, S. Sriram, K. Kalantar-zadeh, M. Bhaskaran, Characterization of metal contacts for two-dimensional MoS_2 nanoflakes, Appl. Phys. Lett. 103 (2013), 232105.
[50] N. Koch, A. Vollmer, A. Elschner, Influence of water on the work function of conducting poly (3, 4-ethylenedioxythiophene)/poly (styrenesulfonate), Appl. Phys. Lett. 90 (2007), 043512.
[51] Y. Tan, L. Chen, F. Wu, B. Huang, Z. Liao, Z. Yu, L. Hu, Y. Zhou, Y. Chen, Regulation of the polar groups in n-type conjugated polyelectrolytes as electron transfer layer for inverted polymer solar cells, Macromolecules 51 (2018) 8197–8204.
[52] G.A. Somorjai, Introduction to Surface Chemistry and Catalysis, Wiley, New York, 1994.
[53] J. Zhang, W. Peng, Z. Chen, H. Chen, L. Han, Effect of cerium doping in the TiO_2 photoanode on the electron transport of dye-sensitized solar cells, J. Phys. Chem. C 116 (36) (2012) 19182–19190.
[54] M. Khannam, S.K. Dolui, Cerium doped TiO_2 photoanode for an efficient quasi-solid state dye sensitized solar cells based on polyethylene oxide/multiwalled carbon nanotube/polyaniline gel electrolyte, Sol. Energy 150 (2017) 55–65, pp.
[55] T.S. Sherkar, L.J.A. Koster, Dielectric effects at organic/inorganic interfaces in nanostructured devices, ACS Appl. Mater. Interfaces 7 (22) (2015) 11881–11889.